

# X-ray selected BALQSOs

M.J. Page<sup>1</sup>, F.J. Carrera<sup>2</sup>, M. Ceballos<sup>2</sup>, A. Corral<sup>3</sup>, J. Ebrero<sup>4</sup>, P. Esquej<sup>5</sup>,  
M. Krump<sup>6</sup>, S. Mateos<sup>2</sup>, S. Rosen<sup>7</sup>, A. Schwoppe<sup>6</sup>, A. Streblyanska<sup>8</sup>,  
M. Symeonidis<sup>1</sup>, J.A. Tedds<sup>7</sup>, M.G. Watson<sup>7</sup>

<sup>1</sup>*Mullard Space Science Laboratory, University College London, Holmbury St Mary, Dorking, Surrey RH5 6NT, UK.*

<sup>2</sup>*Instituto de Física de Cantabria (CSIC–Universidad de Cantabria), 39005 Santander, Spain.*

<sup>3</sup>*IAASARS, National Observatory of Athens, 15236 Penteli, Greece*

<sup>4</sup>*XMM-Newton Science Operations Centre, ESA, Villafranca del Castillo, Apartado 78, 28691 Villanueva de la Cañada, Spain*

<sup>5</sup>*Herschel Science Centre, ESA, Villafranca del Castillo, Apartado 78, 28691 Villanueva de la Cañada, Spain*

<sup>6</sup>*Leibniz-Institut für Astrophysik Potsdam (AIP), An der Sternwarte 16, 14482 Potsdam, Germany*

<sup>7</sup>*Department of Physics and Astronomy, University of Leicester, Leicester, LE1 7RH, UK*

<sup>8</sup>*Instituto de Astrofísica de Canarias (IAC), 38200 La Laguna, Tenerife, Spain*

## ABSTRACT

We study a sample of six X-ray selected broad absorption line (BAL) quasi-stellar objects (QSOs) from the *XMM-Newton* Wide Angle Survey. All six objects are classified as BALQSOs using the classic balnicity index, and together they form the largest sample of X-ray selected BALQSOs. We find evidence for absorption in the X-ray spectra of all six objects. An ionized absorption model applied to an X-ray spectral shape that would be typical for non-BAL QSOs (a power law with energy index  $\alpha = 0.98$ ) provides acceptable fits to the X-ray spectra of all six objects. The optical to X-ray spectral indices,  $\alpha_{OX}$ , of the X-ray selected BALQSOs, have a mean value of  $\langle \alpha_{OX} \rangle = 1.69 \pm 0.05$ , which is similar to that found for X-ray selected and optically selected non-BAL QSOs of similar ultraviolet luminosity. In contrast, optically-selected BALQSOs typically have much larger  $\alpha_{OX}$  and so are characterised as being X-ray weak. The results imply that X-ray selection yields intrinsically X-ray bright BALQSOs, but their X-ray spectra are absorbed by a similar degree to that seen in optically-selected BALQSO samples; X-ray absorption appears to be ubiquitous in BALQSOs, but X-ray weakness is not. We argue that BALQSOs sit at one end of a spectrum of X-ray absorption properties in QSOs related to the degree of ultraviolet absorption in C IV 1550Å.

**Key words:** X-rays: galaxies – quasars: absorption lines

## 1 INTRODUCTION

Broad absorption line (BAL) quasi-stellar objects (QSOs) are a subset of QSOs which show blue-shifted absorption lines with widths  $> 2000 \text{ km s}^{-1}$  in their rest-frame ultraviolet spectra. Most are identified by absorption due to CIV, observed to the blue of the CIV 1550 Å broad emission line. BALQSOs represent between 5 and 20 per cent of the QSO population (Trump et al., 2006; Gibson et al., 2009; Scaringi et al., 2009), with the fraction somewhat dependent on the criteria used to define BALQSOs. It was realised during the 1990s that BALQSOs were systematically fainter in the X-ray band than QSOs without BALs (Green et al., 1995; Green & Mathur, 1996). Since

the launches of *XMM-Newton* and *Chandra*, considerable advances have been made in characterising the X-ray properties of optically-selected BALQSOs (e.g. Gallagher et al., 2006; Morabito et al., 2014), with strong X-ray absorption appearing to be an ubiquitous characteristic of optically-selected BALQSOs.

As might be expected, given their X-ray faintness, BALQSOs are rarely discovered through X-ray sky surveys. Exceptions include one BALQSO found in the *Chandra* Deep Field South (Giacconi et al., 2001), and two discovered during the AXIS survey (Barcons et al., 2002). The largest sample of X-ray selected BALQSOs comes from the  $1^H$  Deep Field, which yielded four such objects (Blustin et al., 2008). The properties of the four  $1^H$  BALQSOs and the CDFS BALQSO were studied in detail

by Blustin et al. (2008). They found that in terms of their rest-frame 2500 Å to 2 keV spectral slopes ( $\alpha_{ox}$ ) the X-ray-selected BALQSOs were a little less X-ray faint than optically-selected BALQSO samples, but still faint in the X-ray compared to X-ray selected non-BAL QSO samples. From the X-ray spectral shapes, Blustin et al. (2008) inferred that the X-ray-selected BALQSOs had similar levels of X-ray absorption to those seen in optically-selected samples of BALQSOs.

Somewhat contradictory results were presented by Giustini et al. (2008), who obtained a sample of 54 X-ray detected BALQSOs by cross-correlating the Sloan Digital Sky Survey (SDSS) Data Release 5 (DR5) QSO catalogue (Schneider et al., 2007) with the Second *XMM-Newton* Serendipitous X-ray Source Catalogue (2XMM; Watson et al., 2009). Giustini et al. (2008) found that one third of the BALQSOs in their sample showed little or no X-ray absorption in their X-ray spectra, and that the distribution of  $\alpha_{OX}$  of their sample was indistinguishable from that of non-BAL QSOs, implying that the BALQSOs in their sample are not X-ray weak.

Subsequently, Streblyanska et al. (2010) compiled a sample of 88 X-ray-detected BALQSOs by cross-correlating the 2XMM catalogue with BALQSOs in the NASA Extragalactic Database (NED). They found that when the X-ray absorption is modelled as ionized gas, as opposed to the neutral absorber model considered by Giustini et al. (2008), 90 per cent of the X-ray detected BALQSOs showed X-ray absorption. Streblyanska et al. (2010) did not examine the  $\alpha_{OX}$  distribution of their BALQSO sample.

It is notable that the X-ray properties found for samples of BALQSOs may depend on the criterion that was used to identify the BALQSOs from their rest-frame UV spectra. A quantitative criterion for classifying an object as a BALQSO was introduced in the form of the balnicity index (BI) by Weymann et al. (1991). For a full definition of balnicity index, see Appendix A of Weymann et al. (1991), but in simple terms it is approximately the equivalent width in  $\text{km s}^{-1}$  of continuous troughs of absorption, with outflow velocities between 3000 and 30000  $\text{km s}^{-1}$  to the blue of CIV  $\lambda 1550$ , and from which the first 2000  $\text{km s}^{-1}$  velocity interval of each absorption trough is excluded from the calculation. Thus  $\text{BI} > 0$  implies at least one absorption trough with a width of  $> 2000 \text{ km s}^{-1}$ . According to Weymann et al. (1991),  $\text{BI} > 0$  is required to classify an object as a BALQSO. An alternative criterion, known as the absorption index (AI), was introduced by Trump et al. (2006), based on an earlier proposal by Hall et al. (2002). In essence, the AI is also an equivalent width measurement, but includes the contribution of absorption troughs with outflow velocities below 3000  $\text{km s}^{-1}$ , and requires a minimum absorption trough width of only 1000  $\text{km s}^{-1}$  to yield a positive AI. Thus  $\text{BI} > 0$  is a more conservative criterion for the classification of BALQSOs than  $\text{AI} > 0$ . Prior to 2006, BALQSOs studied in the X-ray were usually selected by BI, as was the sample studied by Blustin et al. (2008). However the BALQSO sample of Giustini et al. (2008) was based on AI. Streblyanska et al. (2010) selected the sample on AI, but also presented BI values for their sample. They found that while the sources in their sample with  $\text{BI} > 0$  were

almost always absorbed, the sources in their sample with  $\text{BI} = 0$  typically did not have significant X-ray absorption.

In this paper we present a new sample of X-ray selected BALQSOs, which is larger and brighter in X-rays than the sample presented by Blustin et al. (2008). We use the new sample to investigate the X-ray properties of such objects, in particular their optical to X-ray spectral indices and the incidence of X-ray absorbing gas. Throughout, we use the phrase “X-ray selected BALQSOs” specifically for objects which were discovered first as X-ray sources, and then found to be BALQSOs in the subsequent optical spectroscopic follow up. We define power law spectral indices  $\alpha$  such that  $f_\nu \propto \nu^{-\alpha}$ . We have assumed cosmological parameters  $H_0 = 70 \text{ km s}^{-1} \text{ Mpc}^{-1}$ ,  $\Omega_\Lambda = 0.7$  and  $\Omega_m = 0.3$ . Unless stated otherwise, all uncertainties are given at  $1\sigma$ .

## 2 SAMPLE AND UV ABSORPTION PROPERTIES

The sample is drawn from the *XMM-Newton* Wide Angle Survey (XWAS; Esquej et al., 2013), an optical identification programme for X-ray sources, carried out using the 2dF spectrograph (Lewis et al., 2002) on the Anglo-Australian Telescope. The first stage of sample selection involved a visual inspection of XWAS QSOs to identify those which have deep absorption lines blueward of CIV  $\lambda 1550$ . Next, absorption features and parts of the spectra shortward of NV  $\lambda 1250$  were masked, before cross correlating with the QSO template spectrum of Vanden Berk et al. (2001) to obtain redshifts of the objects. Note that for these strong-absorption objects we expect the redshifts obtained by this process to be more accurate than those derived in Esquej et al. (2013). The sample was then refined by measuring the BI of each candidate object. Following Weymann et al. (1991), we consider any object with  $\text{BI} > 0$  to be a BALQSO, and only such objects were included in the final sample, which consists of 6 objects. Their properties are summarised in Table 1, and their optical spectra, as measured in XWAS, are shown in Fig. 1.

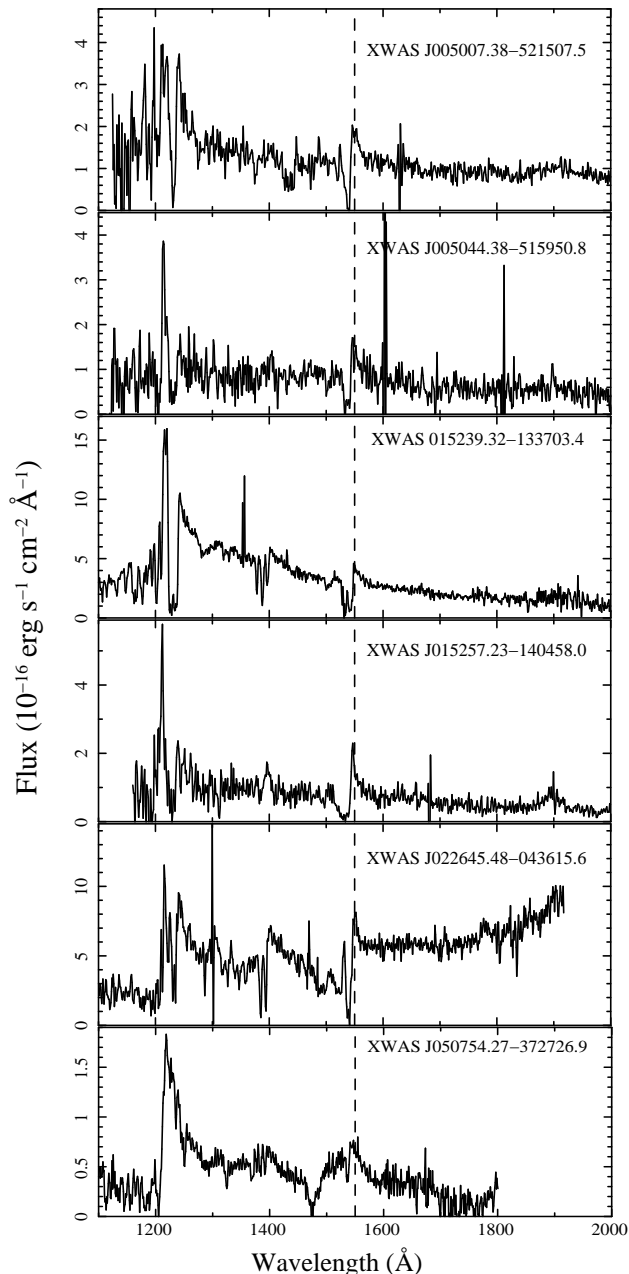
## 3 X-RAY DATA AND CONSTRUCTION OF X-RAY SPECTRA

X-ray spectra were constructed for the BALQSOs using all the *XMM-Newton* European Photon Imaging Camera (EPIC; Strüder et al., 2001; Turner et al., 2001) observations available in the *XMM-Newton* Science Archive. The observations are listed in Table 2. The observations were reduced using standard tasks in the *XMM-Newton* STANDARD ANALYSIS SOFTWARE (SAS) version 14.0<sup>1</sup>, with periods of high background filtered out. Spectra were accumulated from each observation using elliptical source regions with the major axis sized according to the off-axis angle and oriented perpendicular to the off-axis vector to match the point spread function. Background was taken from an annular region around the source, from which

<sup>1</sup> <http://xmm.esac.esa.int/sas>

**Table 1.** List of XWAS BALQSOs and their ultraviolet absorption properties.

Source	IAU name	Redshift	Balnicity Index (km s <sup>-1</sup> )	Outflow Velocity (km s <sup>-1</sup> )	Outflow $\sigma$ (km s <sup>-1</sup> )
XWAS J005007	XWAS J005007.3-521506	2.419 <sup>+0.004</sup> <sub>-0.001</sub>	640 ± 160	-2320 ± 70	560 ± 60
XWAS J005044	XWAS J005044.2-515950	2.479 <sup>+0.006</sup> <sub>-0.002</sub>	120 ± 190	-2800 ± 120	880 ± 80
XWAS J015239	XWAS J015239.2-133703	3.115 ± 0.001	30 ± 40	-2630 ± 80	1470 ± 40
XWAS J015257	XWAS J015257.2-140458	2.314 ± 0.002	890 ± 160	-4200 ± 130	1710 ± 90
XWAS J022645	XWAS J022645.4-043615	3.288 ± 0.001	2450 ± 110	-2090 ± 30	700 ± 30
XWAS J050754	XWAS J050754.2-372726	3.524 ± 0.001	1590 ± 110	-14500 ± 100	1750 ± 80

**Figure 1.** Rest-frame ultraviolet spectra of the X-ray selected BALQSOs. The dashed line marks the rest-frame wavelength of C IV, 1550Å.

circular regions around other sources were excised. Response and effective area files were then constructed for each source and for each EPIC camera, in each observation, using the standard SAS tasks RMFGEN and ARFGEN. Then, the source spectra, background spectra, responses and effective areas for all EPIC cameras and all observations were combined to produce a single source spectrum, background spectrum, response and effective area file for each BALQSO, following the procedure described in Page, Davis & Salvi (2003). Spectra were grouped to a minimum of 20 counts per bin using GRPPHA<sup>2</sup>.

## 4 RESULTS

### 4.1 X-ray spectral analysis

The X-ray spectra of the six BALQSOs are shown in Fig. 2. Analyses of the X-ray spectra were carried out in the spectral fitting package SPEX version 2.02.04<sup>3</sup>. As a first step the spectra were fitted using a power law model, with energy index  $\alpha$  free to vary, and photoelectric absorption from a fixed column density of cold Galactic gas, determined from the Leiden/Argentine/Bonn HI survey (Kalberla et al., 2005). The results are given in Table 3. The best fit slopes  $\alpha$  range from -0.49 to 0.50, significantly below the mean ( $\alpha$ ) = 0.98 for X-ray selected QSOs (Mateos et al., 2005), indicating that the BALQSOs have harder spectral shapes than are usual for QSOs. For five of the six BALQSOs the simple power law fit provides an acceptable goodness of fit (null hypothesis probability > 1 per cent), but the fit is poor for XWAS J005007.

A deficiency of soft X-rays is commonly a sign of absorption, so we have considered an alternative model consisting of a power law with ionized absorption as well as absorption from cold Galactic material. As before, the Galactic  $N_H$  was fixed. This time, we fixed the power law slope to  $\alpha = 0.98$ . For the ionized absorption, we used the XABS model in SPEX, which predicts both bound-bound and bound-free absorption from an equilibrium photoionized plasma for which the ionization state is characterised by the ionization parameter  $\xi$ . The XABS model assumes an ionizing continuum shape based on the type 1 AGN NGC 5548 (Steenbrugge et al., 2005) and a Gaussian velocity dispersion for the absorber. With respect to the rest-frame of the QSO, we assume that the absorber seen in the X-ray band has a similar outflow velocity and

<sup>2</sup> <http://heasarc.nasa.gov/docs/software/ftools>

<sup>3</sup> <http://www.sron.nl/divisions/hea/spex/index.html>

**Table 2.** Galactic column densities for the BALQSOs and *XMM-Newton* observations used in the construction of the X-ray spectra. Column densities are taken from the Leiden/Argentine/Bonn Survey of Galactic HI (Kalberla et al., 2005). The column labelled “Counts” gives the total number of net (i.e. background-subtracted) 0.2–12 keV counts used in the combined EPIC spectrum for each source.

Source	$N_H$ ( $10^{20} \text{ cm}^{-2}$ )	Counts	Obs ID	pn	Filters		Exposure time (ks)		
					MOS1	MOS2	pn	MOS1	MOS2
XWAS J005007	2.58	197	0123920101	Medium	-	-	14.9	-	-
			0125320401	Medium	Medium	Medium	17.0	21.4	21.4
			0125320501	Thin	Medium	Medium	3.5	6.3	6.2
			0125320701	Medium	Thin	Thin	10.5	14.8	14.7
			0133120301	Thin	Thin	Thin	6.5	10.7	10.7
			0133120401	Thin	Thin	Thin	7.3	10.7	10.6
			0153950101	-	Thin	Thin	-	4.5	4.5
XWAS J005044	2.39	133	0123920101	Medium	-	-	15.4	-	-
			0125320401	Medium	Medium	Medium	17.0	21.4	21.4
			0125320501	Thin	Medium	Medium	3.5	6.2	6.2
			0125320701	Medium	Thin	Thin	10.5	14.8	14.7
			0133120301	Thin	Thin	Thin	6.5	10.7	10.7
			0133120401	Thin	Thin	Thin	7.3	10.7	10.6
			0153950101	Medium	-	Thin	1.7	-	4.5
XWAS J015239	1.54	341	0112300101	Thin	Thin	Thin	16.1	24.6	25.7
			0602010101	Thin	Thin	Thin	71.1	87.3	87.7
XWAS J015257	1.29	72	0109540101	Medium	Medium	Medium	42.0	53.0	52.9
XWAS J022645	2.31	78	0112681301	Thin	Thin	Thin	9.6	16.7	16.7
XWAS J050754	2.61	237	0110980801	Thin	Thin	Thin	30.1	39.0	39.2

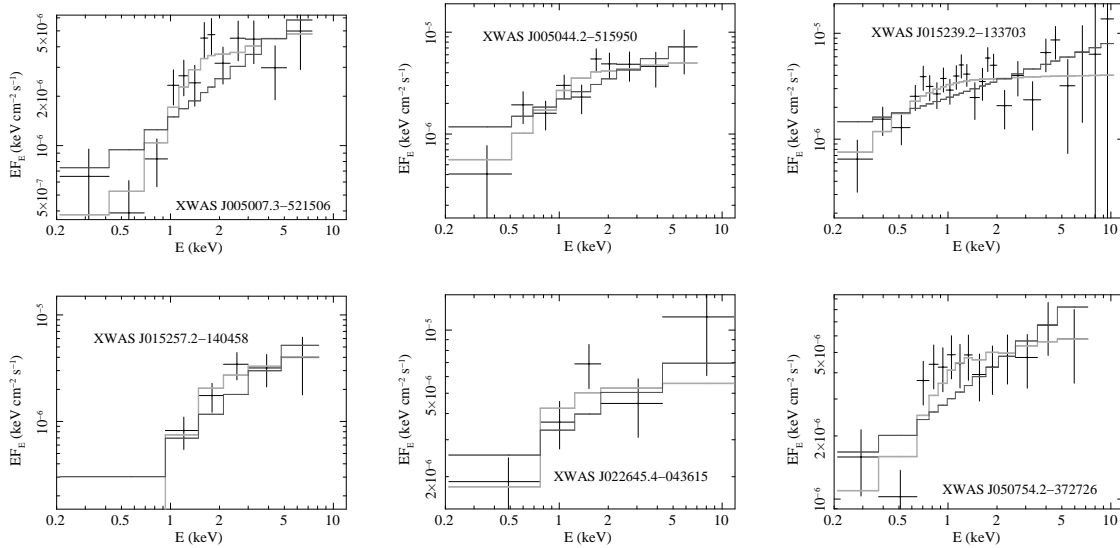


**Figure 2.** *XMM-Newton* EPIC spectra of the six BALQSOs. The spectra have been flux calibrated by dividing through by the product of the effective area and Galactic transmission and are shown as  $EF_E$ . A power law with  $\alpha = 1$  would be a horizontal line. The dark stepped lines show the power law model (model PL in Table 3) while the light-grey stepped lines show the model including an ionized absorber (model PL  $\times$  IA in Table 3).

velocity dispersion as the UV absorber. Therefore, appropriate parameters were determined from Gaussian fits to the main C IV absorbing trough in each restframe UV spectrum, and are given in Table 1.

The power law and ionized absorber model provides acceptable fits for all 6 BALQSO spectra. Confidence con-

tours for  $\log \xi$  and  $\log N_H$  of the absorbers, as derived from the X-ray fits are shown in Fig. 3. The ionization parameters of the absorbers are poorly constrained from the fits, and somewhat correlated with the column densities. Nonetheless, robust lower limits on the column densities of between  $10^{22}$  and  $10^{23} \text{ cm}^{-2}$  can be inferred from Fig. 3

**Table 3.** Results of spectral fitting. The models are a power law (labelled PL), and a power law attenuated by an ionized absorber, with the power law index fixed at  $\alpha_X = 0.98$  (labelled PL  $\times$  IA). In both cases a photoelectric absorber with fixed column density was included to represent Galactic absorption.  $P$  is the null hypothesis probability corresponding to  $\chi^2/\nu$ . An asterisk is used to indicate parameter uncertainties for which the limits of the fitting range were reached before  $\Delta \chi^2 = 1$ .

	XWAS J005007	XWAS J005044	XWAS J015239	XWAS J015257	XWAS J022645	XWAS J050754
PL						
$\alpha_X$	$0.12 \pm 0.10$	$0.14 \pm 0.14$	$0.47 \pm 0.08$	$-0.45 \pm 0.20$	$0.39 \pm 0.18$	$0.40 \pm 0.09$
$\chi^2/\nu$	26.4/11	9.6/8	37.9/23	8.9/4	4.4/3	22.5/12
$P$	0.0057	0.29	0.026	0.064	0.22	0.032
PL $\times$ IA						
$\log \xi$	$2.8^{+0.3}_{-0.5}$	$2.6^{+0.4}_{-2.6*}$	$0.0^{+2.5}_{-0.0*}$	$2.6^{+0.6}_{-2.6*}$	$1.1^{+2.7}_{-1.1*}$	$2.8^{+0.4}_{-2.8*}$
$\log N_H$	$23.6^{+0.3}_{-0.3}$	$23.3^{+0.4}_{-0.5}$	$22.5^{+0.5}_{-0.1}$	$23.9^{+0.4}_{-0.6}$	$22.7^{+0.6}_{-0.3}$	$23.4^{+0.4}_{-0.6}$
$\chi^2/\nu$	8.8/10	6.9/7	21.7/22	1.0/3	3.3/2	9.3/11
$P$	0.56	0.43	0.48	0.31	0.19	0.60

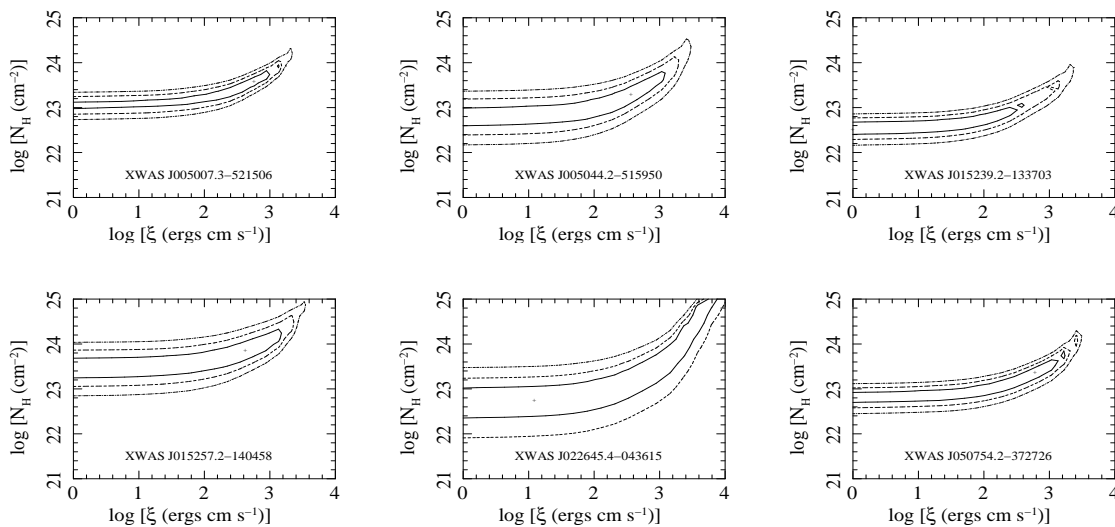


**Figure 3.** Confidence contours for  $\xi$  and  $N_H$  in the ionized absorber model fits to the *XMM-Newton* spectra. The small cross indicates the best-fitting parameter values. Solid, dashed and dot-dashed contours correspond to 68, 95 and 99.73 per cent confidence for 2 interesting parameters.

for all of the objects except XWAS J022645, which has the poorest quality X-ray spectrum.

## 4.2 X-ray to optical ratio

Following the usual convention in AGN studies, we have parameterised the X-ray to optical flux ratio of our BALQSOs as  $\alpha_{OX}$ , the power law slope which would connect the flux densities at 2500 Å and 2 keV in the rest-frame of the source. The 2 keV flux measurements were derived from the power law model fits to the X-ray spectra without ionised absorbers (i.e. model PL in Table 3), similar to the approach taken by Gallagher et al. (2006) and Blustin et al. (2008). The rest-frame 2500 Å flux was derived from  $R$  band magnitudes measured by the SuperCOSMOS Sky Survey (Hambly et al., 2001a) scans of the UK Schmidt Telescope  $R$  plates, converted to monochromatic flux densities assuming the template spectrum of Vanden Berk et al. (2001). Uncertainties on the  $R$  magnitudes are taken from Table 6 of Hambly et al. (2001b).

Uncertainties on  $\alpha_{OX}$  were derived by propagating the statistical uncertainties on the X-ray model fits and  $R$  magnitudes. The values of  $\alpha_{OX}$  are given in Table 4, together with broadband fluxes and magnitudes.

## 5 DISCUSSION

The X-ray spectra of the BALQSOs show significant evidence for absorption. Although the majority of the X-ray spectra can be successfully fitted with power-law models without intrinsic absorption, the derived spectral indices ( $-0.5 < \alpha_X < 0.5$ ) are significantly lower than the norm for non-BAL QSOs, which cluster around a mean of  $\langle \alpha_X \rangle = 0.98$  with a dispersion of  $\sigma_\alpha = 0.27$  (Mateos et al., 2005, 2010; Scott et al., 2011), indicating that the BALQSOs have significantly harder shapes than non-BALQSOs. All of the spectra can be fitted successfully with a model in which a typical non-BAL QSO spectrum passes through an ionized absorber. The six sources presented here therefore have X-ray spectral properties

**Table 4.** Magnitudes, broadband fluxes and  $\alpha_{OX}$ . The  $R$  magnitudes come from the SuperCOSMOS Sky Survey scans of the UK Schmidt Telescope  $R$  plates. Extinction estimates come from the Schlafly & Finkbeiner (2011) calibration of the Schlegel et al. (1998) dust maps. The 0.5–2.0 keV flux values are derived from the power law spectral fits without any intrinsic absorption (model PL in Table 3). The column headed ‘ $\alpha_{OX}$  observed’ gives the values of  $\alpha_{OX}$  in which the rest-frame 2 keV flux is derived from the power law fits (model PL in Table 3), while the column headed ‘ $\alpha_{OX}$  corrected’ gives values of  $\alpha_{OX}$  in which the rest-frame 2 keV flux is derived from the power law continuum in the ionized absorber model (model PL  $\times$  IA in Table 3), with no attenuation from the ionized absorption. The column headed ‘ $\alpha_{OX}$  predicted’ gives the values of  $\alpha_{OX}$  that would be predicted from the 2500 Å monochromatic luminosities and equation 3 from Just et al. (2007).

Source	$R$ (mag)	$A_R$ (mag)	0.5–2.0 keV flux ( $10^{-15}$ erg cm $^{-2}$ s $^{-1}$ )	$\alpha_{OX}$ observed	$\alpha_{OX}$ corrected	$\alpha_{OX}$ predicted
XWAS J005007	$19.51 \pm 0.13$	0.04	$3.25 \pm 0.34$	$1.75 \pm 0.03$	$1.41^{+0.08}_{-0.07}$	1.62
XWAS J005044	$20.69 \pm 0.18$	0.04	$4.70 \pm 0.62$	$1.49 \pm 0.04$	$1.20^{+0.08}_{-0.16}$	1.56
XWAS J015239	$19.14 \pm 0.13$	0.04	$5.57 \pm 0.41$	$1.68 \pm 0.03$	$1.52^{+0.03}_{-0.03}$	1.67
XWAS J015257	$20.44 \pm 0.18$	0.03	$1.26 \pm 0.32$	$1.87 \pm 0.06$	$1.33^{+0.11}_{-0.25}$	1.57
XWAS J022645	$18.87 \pm 0.11$	0.06	$7.46 \pm 1.10$	$1.67 \pm 0.04$	$1.52^{+0.05}_{-0.13}$	1.70
XWAS J050754	$19.13 \pm 0.13$	0.07	$6.68 \pm 0.54$	$1.70 \pm 0.03$	$1.46^{+0.06}_{-0.07}$	1.69

which are consistent with those of the five X-ray selected BALQSOs studied by Blustin et al. (2008).

On the other hand, the observed ultraviolet to X-ray spectral slopes  $\alpha_{OX}$  of our six X-ray selected BALQSOs are quite consistent with those expected for non-BAL QSOs. There is a well-known relation between ultraviolet luminosity and  $\alpha_{OX}$  in non-BAL QSOs (Strateva et al., 2005; Steffen et al., 2006; Just et al., 2007). The relation holds for both optically-selected and X-ray selected non-BAL QSO samples (Lusso et al., 2010). Using the expression from Just et al. (2007),  $\alpha_{OX} = 0.14(\log L_\nu) + 2.705$  where  $L_\nu$  is the monochromatic luminosity at 2500Å, we have calculated the predicted  $\alpha_{OX}$  values (see Table 4). Taking into account the observed scatter around this relation of  $\sigma_\alpha = 0.14$  (Just et al., 2007), we would predict a mean of  $\langle\alpha_{OX}\rangle = 1.64 \pm 0.06$  for our sample of objects if they were non-BAL QSOs, which is quite consistent with the observed  $\langle\alpha_{OX}\rangle = 1.69 \pm 0.05$ . In contrast, optically-selected samples of BALQSOs usually show much larger values of  $\alpha_{OX}$  than our X-ray-selected sample. For example the majority of the sample of 36 BALQSOs from the Large Bright Quasar Survey studied by Gallagher et al. (2006) have  $\alpha_{OX} > 2$ , and their  $\langle\alpha_{OX}\rangle$  is larger by 0.52 than the mean that would be expected given their ultraviolet luminosities.

At first sight, finding that our BALQSOs have  $\alpha_{OX}$  values in the normal range for non-BAL QSOs seems at odds with the presence of significant X-ray absorption in their X-ray spectra, because the X-ray absorption would be expected to lead to increased  $\alpha_{OX}$  compared to a typical QSO without significant X-ray absorption. An explanation can be gleaned by examining how the absorption should affect  $\alpha_{OX}$ . For each of our BALQSOs we have recalculated the  $\alpha_{OX}$  using the intrinsic (i.e. unabsorbed) rest-frame 2 keV model continuum from the ionized absorber model fits in Table 3. These absorption-corrected values are given in Table 4 in the column headed ‘ $\alpha_{OX}$  corrected’. In all cases the absorption-corrected  $\alpha_{OX}$  values are lower than those predicted by the Just et al. (2007) relation by between 1 and 3 times the scatter (0.14) found by Just et al. (2007). Therefore

intrinsically, these objects occupy the lowest 15 per cent of the  $\alpha_{OX}$  distribution.

In constructing an X-ray selected BALQSO sample we have naturally selected BALQSOs which are at the X-ray-bright end of the distribution. As such we would expect to find the part of the population with the lowest levels of X-ray absorption, and/or the smallest intrinsic values of  $\alpha_{OX}$ . We do not find any examples of BALQSOs without strong X-ray absorption, but all of our sample have intrinsic  $\alpha_{OX}$  values which are low compared to the majority of QSOs at similar UV luminosities.

Consistent with our findings, Blustin et al. (2008) also found evidence for strong X-ray absorption in the X-ray spectra of all of their X-ray selected BALQSOs. The values of  $\alpha_{OX}$  found by Blustin et al. (2008) are a little higher than for the six objects in our sample, though still much lower than typically found for optically selected BALQSOs. Observationally, the sample of Blustin et al. (2008) was selected from deep X-ray surveys, whereas ours is drawn serendipitously from moderate exposure ( $< 50$  ks) XMM-Newton observations. The mean 0.5–2 keV flux of the Blustin et al. (2008) sample is 5 times lower than the mean 0.5–2 keV flux of the six sources studied here, and the mean 0.5–2 keV luminosity of the Blustin et al. (2008) sample is 7 times lower than the mean 0.5–2 keV luminosity of the six sources studied here. By selecting BALQSOs at a higher X-ray flux limit than Blustin et al. (2008), we have been able to push further into the X-ray-bright end of the BALQSO population, and so are able to draw stronger conclusions regarding their X-ray properties. Our findings suggest that X-ray absorption is a universal property of BALQSOs, but imply that X-ray weakness (i.e. large  $\alpha_{OX}$ ) is not.

In the study of Streblyanska et al. (2010) there were two notable correlations concerning the X-ray absorbers, which Streblyanska et al. (2010) modelled as ionized absorbers. First, they found a correlation between the ionization parameter  $\xi$  and  $N_H$ , and second they found a correlation between  $N_H$  and the BI of the ultraviolet absorption. Our sample is too small to permit such a correlation analysis, but our spectral fitting may provide some insights into these correlations. It is clear from Fig. 3 that with the current statistics in our X-ray spectra, the ionization param-

eters of the absorbers are not constrained, and there is significant covariance between  $\log \xi$  and  $\log N_H$  in the individual spectral fits. The six BALQSOs in our sample show a consistent trend in correlation between  $\log \xi$  and  $\log N_H$  to that found by Streblyanska et al. (2010), but it can be accounted for entirely by this covariance. The ionized absorption model we have used, XABS in SPEX, is more sophisticated than that used by Streblyanska et al. (2010), ABSORI in XSPEC (Arnaud, 1996), because XABS includes bound-bound transitions as well as bound-free transitions, while ABSORI includes only bound-free transitions. However, we would expect a similar level of covariance between  $\log \xi$  and  $\log N_H$  in the two models.

Most of the BALQSOs in the sample of Streblyanska et al. (2010) for which spectral fitting has been performed are brighter in X-rays than those in our sample, so the degeneracy between  $\xi$  and  $N_H$  may be mitigated to some extent by the improved photon statistics compared to our sample, but it is nonetheless a concern that some or all of the correlation found by Streblyanska et al. (2010) between  $\xi$  and  $N_H$  may be a consequence of the covariance of these two parameters.

Of the correlation found by Streblyanska et al. (2010) between BI and  $N_H$  we can neither confirm nor refute this correlation with our small sample. Some insight on the relation between ultraviolet CIV absorption and X-ray absorption in QSOs may be drawn by comparing our sample of BALQSOs with the X-ray absorbed QSOs studied by Page et al. (2011). Comparison of Fig. 3 with the corresponding figure 4 in Page et al. (2011) (and disregarding the object RX J124913 from their sample, which is itself a BALQSO), we find that the X-ray absorbed QSOs have confidence contours in  $(\log \xi, \log N_H)$  which fall systematically below those of our BALQSO sample. Despite the degeneracy between  $\xi$  and  $N_H$  in both samples, the X-ray selected BALQSOs have systematically more X-ray absorption than the X-ray absorbed QSOs, which were also X-ray selected. The X-ray absorbed QSOs of Page et al. (2011) also have lower CIV equivalent widths than the BALQSOs. There thus appears to be a continuous spectrum of QSO absorption properties, from the majority of QSOs which have CIV equivalent widths of  $< 5 \text{ \AA}$  and minimal X-ray absorption, through the X-ray absorbed QSOs which typically have CIV equivalent widths in the range of  $5 - 20 \text{ \AA}$  and moderate X-ray absorption, to the BALQSOs which have CIV equivalent widths  $> 20 \text{ \AA}$  and the strongest X-ray absorption. A similar correlation between CIV equivalent width and  $\alpha_{OX}$  has long been established (Brand, Laor & Wills, 2000). As X-ray absorption appears to be a universal property of BALQSOs but large  $\alpha_{OX}$  is not, the connection between CIV absorption and X-ray absorption may be considered more fundamental than that between CIV and  $\alpha_{OX}$ .

Significant X-ray absorption, with  $\log N_H > 10^{22.5} \text{ cm}^{-2}$  appears to be a ubiquitous property amongst X-ray selected BALQSOs, defined according to the classical BI  $> 0$  criterion, as presented here and by Blustin et al. (2008). The same conclusion was reached by Streblyanska et al. (2010) for BALQSOs identified by correlating optical catalogues with the 2XMM catalogue. We are thus led to the same conclusion as Streblyanska et al. (2010) that the rather different ab-

sorption properties found by Giustini et al. (2008) for X-ray detected BALQSOs, probably relates to their use of the AI definition of BALQSOs. The AI criterion used by Giustini et al. (2008) includes objects with lower CIV equivalent widths than the classical BI criterion, and this may account for the comparatively weak X-ray absorption found by those authors for some of their sample. The apparent difference in X-rays between BALQSOs defined by BI and those defined by AI (and not BI) is interesting in the context of the bimodality of the AI distribution demonstrated by Knigge et al. (2008) and their interpretation that the bimodality corresponds to two distinct sub-populations of QSOs. It appears that the two sub-populations selected by AI have distinct distributions in X-ray absorption, as well as in their UV absorption-line properties.

## 6 CONCLUSIONS

We have presented a sample of six X-ray selected BALQSOs from XWAS. Examination of their X-ray spectra indicates that all have hard spectral shapes compared to the majority of QSOs, suggesting absorption. An ionized absorption model applied to a typical AGN template X-ray spectrum is able to reproduce the X-ray spectral shapes, and implies that these are intrinsically rather X-ray bright for QSOs given their UV luminosities. X-ray absorption appears to be ubiquitous in classically-defined (i.e. BI  $> 0$ ) BALQSOs, and this is true for X-ray-selected BALQSOs as well as for optically-selected samples. In contrast, X-ray weakness (i.e. high  $\alpha_{OX}$ ) is not a universal property of BALQSOs. We have argued that there is a continuous spectrum of X-ray absorption properties in QSOs which are related to the equivalent width of ultraviolet CIV absorption, with BALQSOs forming the most heavily absorbed end of the distribution.

## 7 ACKNOWLEDGMENTS

Based on observations obtained with *XMM-Newton*, an ESA science mission with instruments and contributions directly funded by ESA Member States and NASA. This research was also based on observations made at the Anglo-Australian Telescope. MJP acknowledges financial support from the UK Science and Technology Facilities Council. FJC and SM acknowledge financial support through grant AYA2015-64346-C2-1-P (MINECO/FEDER). MTC acknowledges support by the Spanish Programa Nacional de Astronomía y Astrofísica under grant AYA2009-08059. MK acknowledges support by DFG grant KR 3338/3-1. The NASA/IPAC Extragalactic Database (NED) is operated by the Jet Propulsion Laboratory, California Institute of Technology, under contract with the National Aeronautics and Space Administration.

**REFERENCES**

- Arnaud K.A., 1996, *Astronomical Data Analysis Software and Systems V*, eds. Jacoby G. and Barnes J., ASP Conf. Series volume 101, p17
- Barcons X., et al., 2002, *A&A*, 382, 522
- Blustin A.J., et al., 2008, *MNRAS*, 390, 1229
- Brandt W.N., Laor A. & Wills B.J., 2000, *ApJ*, 528, 637
- Esquej P., et al., 2013, *A&A*, 577, A123
- Gallagher S.C., Brandt W.N., Chartas G., Priddey R., Garmire G.P., Sambruna R.M., 2006, *ApJ*, 644, 709
- Giacconi R., et al., 2001, *ApJ*, 551, 624
- Gibson R.R., et al., 2009, *ApJ*, 692, 758
- Giustini M., Cappi M., Vignati C., 2008, *A&A*, 491, 425
- Green P.J., 1995, *ApJ*, 450, 51
- Green P.J. & Mathur S., 1996, *ApJ*, 462, 637
- Hall P.B., et al., 2002, *ApJS*, 141, 267
- Hambly N.C., et al., 2001, *MNRAS*, 326, 1279
- Hambly N.C., Irwin M.J., MacGillivray H.T., 2001, *MNRAS*, 326, 1295
- Just D.W., Brandt W.N., Shemmer O., Steffen A.T., Schneider D.P., Chartas G., Garmire G.P., 2007, *ApJ*, 665, 1004
- Kalberla P.M.W., Burton W.B., Hartman Dap, Arnal E.M., Bajaja E., Morras R., Pöppel W.G.L., 2005, *A&A*, 440, 775
- Knigge C., Scaringi S., Goad M.R., Cottis C.E., 2008, *MNRAS*, 386, 1426
- Lewis I.J., et al., 2002, *MNRAS*, 333, 279
- Lusso E., et al., 2010, *A&A*, 512, A34
- Mateos S., et al., 2005, *A&A*, 433, 855
- Mateos S., et al., 2010, *A&A*, 510, 35
- Morabito L.K., Dai X., Leighly K.M., Sivakoff G.R., Shankar F., 2014, *ApJ*, 786, 58
- Page M.J., Davis S.W. & Salvi N.J., 2003, *MNRAS*, 343, 1241
- Page M.J., Carrera F.J., Stevens J.A., Ebrero J., Blustin A.J., 2011, *MNRAS*, 416, 2792
- Scaringi S., Cottis C.E., Knigge C., Goad M.R., 2009, *MNRAS*, 399, 2231
- Schlaflly E.F. & Finkbeiner D.P., 2011, *ApJ*, 737, 103
- Schlegel D.J., Finkbeiner D.P., Davis M., 1998, *ApJ*, 500, 525
- Schneider D.P., et al., 2007, *AJ*, 134, 102
- Scott A., Stewart G.C., Mateos S., Alexander D.M., Hutton S., Ward M.J., 2011, *MNRAS*, 417, 992
- Steenbrugge K.C., et al., 2005, *A&A*, 434, 569
- Steffen A.T., Strateva I., Brandt W.N., Alexander D.M., Koekemoer A.M., Lehmer B.D., Schneider D.P., Vignali C., 2006, *AJ*, 131, 2826
- Strateva I.V., Brandt W.N., Schneider D.P., Vanden Berk D.G., Vignali C., 2005, *AJ*, 130, 387
- Streblyanska A., Barcons X., Carrera F.J., Gil-Merino R., 2010, *A&A*, 515, A2
- Strüder L., et al., 2001, *A&A*, 365, L18
- Trump J.R., et al., 2006, *ApJS*, 165, 1
- Turner M.J., et al., 2001, *A&A*, 365, L27
- Vanden Berk D.E., et al., 2001, *AJ*, 122, 549
- Watson M.G., et al., 2009, *A&A*, 493, 339
- Weymann R.J., Morris S.L., Foltz C.B., Hewett, P.C., 1991, *ApJ*, 373, 23